Original article

Laser-assisted grinding of reaction-bonded SiC

Journal of Micromanufacturing
3(2) 93–98, 2020

DOI: 10.1177/2516598420965342
journals.sagepub.com/home/jmf


Xichun Luo[1], Zhipeng Li[2], Wenlong Chang[1], Yukui Cai[1], Jining Sun[3], Fei Ding[1], Feihu Zhang[2], Haitao Liu[2] and Yazhou Sun[2]

Abstract

The article presents the development of a novel laser-assisted grinding (LAG) process to reduce surface roughness and subsurface damage in grinding reaction-bonded silicon carbide (RB-SiC). A thermal control approach is proposed to facilitate the process development, in which a two-temperature model (TTM) is applied to control the required laser power to thermal softening of RB-SiC prior to the grinding operation without melting the workpiece or leaving undesirable microstructural alteration. Fourier's law is adopted to obtain the thermal gradient for verification. An experimental comparison of conventional grinding and LAG shows significant reduction of machined surface roughness (37%–40%) and depth of subsurface damage layer (22%–50.6%) using the thermal control approach under the same grinding conditions. It also shows high specific grinding energy 1.5 times that in conventional grinding at the same depth of cut, which accounts for the reduction of subsurface damage as it provides enough energy to promote ductile-regime material removal.

Keywords

Grinding, silicon carbide, laser-assisted, thermal control, subsurface damage

Introduction

Due to its superb properties such as chemical inertness, high carrier saturation velocity, high temperature resistance and high specific stiffness, silicon carbide (SiC) is regarded as a promising material to replace silicon for the next generation of power electronics, quantum computing and semiconductor devices. However, it is one of the hardest-to-machine materials due to the high hardness and brittleness. Ductile-regime diamond grinding is an important manufacturing technique in the process chain for SiC, which usually delivers sub-micron-level ground surface roughness with depth of subsurface damage of several microns. Time-consuming polishing, therefore, has to be employed to further improve surface roughness down to the nanometer level and remove subsurface damage layer. As a result, production cost of a SiC wafer is several times higher than that of a Si wafer of the same size. This has hindered the further development of SiC technology and its commercialization.

In recent years, ultrasonic-assisted grinding has been developed to improve surface roughness in grinding brittle materials. Research shows that with ultrasonic frequency vibration of the grinding wheel, the critical depth of cut can be increased, which enhances the ductile regime grinding condition and results in reduced surface roughness.[1] As the mechanical stress of materials normally decreases with increase of temperature due to thermal softening,[2] laser-assisted grinding (LAG) has also been attempted to machine brittle materials, in which 30% reduction in surface roughness was achieved compared with conventional grinding.[3] Very recently, a novel LAG process that used lasers for micro-structuring silicon nitride (Si_3N_4) ceramics improved material removal rate while slightly improving ground surface quality.[4]

Wang et al.[5] revealed that the machined surface quality in laser-assisted machining (LAM) of Al_2O_3p/Al could be improved and the tool wear could be reduced by 20%–30% compared with conventional cutting. On the other hand, in LAM of Al_2O_3 ceramics, Chang and Kuo[6] found that the feed and thrust cutting forces could be reduced by 22% and 20%, respectively. Also, Guerrini et al.[7] induced thermal cracks by laser radiation before grinding sintered reaction Si_3N_4, which again showed that the average force decreased by 26%–27%. The researcher focused not just on the machining force, as the material removal mechanism of LAM was another

[1] Centre for Precision Manufacturing, DMEM, University of Strathclyde, Glasgow, UK
[2] School of Mechatronics, Harbin Institute of Technology, Harbin, PR China
[3] School of Engineering and Physical Science, Heriot-Watt University, Edinburgh, UK

Corresponding author:
Xichun Luo, Centre for Precision Manufacturing, DMEM, University of Strathclyde, Glasgow G11XJ, UK.
E-mail: Xichun.luo@strath.ac.uk

key research area. The surface of the Si_3N_4 workpiece was oxidized to form an amorphous silicate, which could reduce the hardness and, finally, promote the material removal rate and benefit the tool wear.[8] However, these above studies mostly focused on the reduction of machined surface roughness, forces and removal mechanism. Studies on new process controls to minimize subsurface damage are rare. In fact, the level of subsurface damage is a significant surface quality characterization parameter, as it influences the performance of the final products. In LAG, control of the preheat level is crucial to success.

In this study, a thermal control approach is proposed to facilitate the development of a novel LAG process for RB-SiC. An experimental study is carried out to evaluate the effectiveness of this approach in comparison with conventional grinding in relation to surface roughness and depth of subsurface damage layer of the ground RB-SiC. The mechanism of laser preheating on the reduction of subsurface damage is investigated from the point of view of specific grinding energy.

Thermal control in laser-assisted grinding

In LAG, the material removal temperature T_s, which is defined as the average temperature of the material as it enters the grinding zone, plays an important role. It has to be controlled precisely to achieve the full benefits of LAG without melting the workpiece or leaving undesirable microstructural alteration in the machined workpiece.

During laser preheating, the laser thermal energy is first absorbed by the electrons in the SiC. After that, the thermal energy is transferred from the electrons to the lattices of the SiC by thermal conduction, although some energy is lost due to thermal diffusion. Laser energy density and laser power are two critical laser machining parameters to be controlled in LAG. The study adopts a two-temperature model (TTM) to obtain them. In this model, the electrons and lattices are treated as two separate heat baths with temperature T_e and T_l, respectively. The diffusion equation between the electrons and the lattices can be described as[9]:

$$C_e \frac{\partial T_e}{\partial t} = -\frac{\partial Q(z)}{\partial z} - \gamma (T_e - T_l) + S \tag{1}$$

$$C_l \frac{\partial T_l}{\partial t} = \gamma (T_e - T_l) \tag{2}$$

where C_e, C_l, and z are the heat capacities of the electron and the lattice, and the ablation rate to SiC, respectively. $Q(z)$ is the electron heat flux, and it can be calculated as: $Q(z) = -k_e \partial T_e / \partial z$. k_e is the electron thermal conductivity. S is the absorbed energy. The electrons and lattices are in thermal equilibrium state, i.e., $T_e = T_l$. Therefore, Equation (1) can be simplified as:

$$C_e \frac{\partial T_e}{\partial t} - \frac{-\mathrm{ke}\partial T\mathrm{e} / \partial z}{\partial z} = S. \tag{3}$$

The absorbed energy S in Equation (3) can be expressed as:

$$S = I(t) A_b \alpha e^{-\alpha z} \tag{4}$$

where $I(t)$ is the laser intensity. A_b and α are the surface transmissivity and optical penetration depth of RB-SiC, respectively. The temperature of the electrons can be described by integration of Equation (1):

$$T_e = \left[\frac{2I(t) At \alpha \mathrm{e}^{-\alpha z}}{\dot{C}_e} \right]^{\frac{1}{2}} \tag{5}$$

The temperature of the lattice can be simplified as $(T_i \approx T_e t / C_i$. As it can also be determined by the average cooling time of the electrons $(t = C`_e T_e / 2)$, it will have

$$T_i \approx T_e^2 \frac{C`_e}{2C_i} \approx \frac{F\alpha}{C_i} \mathrm{e}^{-\alpha z} \tag{6}$$

where F is the laser energy density. The ablation threshold, $F_0 \approx T_l C_l / \alpha$ can be described by the Arrhenius-type equation. Equation (6) can be written as:

$$F \approx F_0 \mathrm{e}^{-\alpha z} \tag{7}$$

The ablation threshold and the optical penetration depth for SiC are 1.5 J/cm^2 and 1.7 μm^{-1}, respectively. The ablation rate is 1.8 μm/pulse. Therefore, the energy density can be obtained through Equation (7) as 0.07 J/cm^2.

According to the definition of the energy density, the power of the laser system (P) to be used in the laser deburring process can be obtained as:

$$P = F F_r A \tag{8}$$

where F_r and A are the laser frequency and area of the laser spot, respectively.

A laser wavelength of 1064 nm is used with a laser spot of 4 mm diameter. The calculated maximum laser power below the laser ablation threshold is 88 W.

As laser preheating will always result in non-steady-state heat conduction, the surface temperature heated by the laser can be calculated by Fourier's law, which can be described as:

$$\nabla^2 T = \frac{\rho c}{k} \frac{\partial T}{\partial t} - \frac{A_v I(x, y, z, t)}{k} \tag{9}$$

where T is the temperature of the workpiece, and ρ and c are the density and the specific heat of the workpiece, respectively. k is the thermal diffusivity of the workpiece. A_v is the fraction of the radiation energy absorbed per unit volume of the workpiece, and I is the Gaussian distribution of the intensity.

It is assumed that in an LAG process, radiation and convection are not significant sources of heat loss and are therefore negligible. The complete solution for the uniform constant irradiance is:

$$T\left(z_c,t\right)=\frac{2I_0}{k}\left[\left(\frac{\kappa t}{\pi}\right)^{\frac{1}{2}}\mathrm{e}^{\left(-z_c^2/4\kappa t\right)}-\frac{z_c}{2}\mathrm{erfc}\frac{z_c}{\sqrt{4\kappa t}}\right] \quad (10)$$

where

$$\kappa=\frac{k}{\rho c} \quad (11)$$

$$\mathrm{erf}\left(s\right)=\frac{2}{\sqrt{\pi}}\int_0^s \mathrm{e}^{-x^2}dx \quad (12)$$

where erf(s) is the error function and erfc(s) is the complementary error function equal to 1 − erf(s). I_0 is the irradiance, and z_c is the depth coordinate radiated into the sample. The surface temperature of the semi-infinite solid is given by:

$$T_s\left(0,t\right)=\frac{I_0}{k}\left(\frac{4\kappa t}{\pi}\right)^{1/2} \quad (13)$$

Equation (13) shows that the temperature rise is caused by releasing the heat (F_q) per unit area. Note that for very long heating durations ($t\rightarrow\infty$), the temperature increases on the surface, and $T\sim\sqrt{t}$ would be unlimited. This is useful for estimating the time required to reach a specified surface temperature for a given laser irradiation. The material properties of RB-SiC shown in Table 1 have been used in the calculations.

Table 1. Material property of RB-SiC in this study.

Items	RB-SiC
Elastic modulus (GPa)	390
Vickers hardness (k f·mm^{-2})	3,000
Compressive strength (MPa)	2,000
Fracture toughness (K_{IC}) (MPa·m$^{1/2}$)	4.0
Thermal expansion coefficient (×10^{-6}/°C)	3
Thermal conductivity (W/mK)	150
Thermal shock resistance (°C)	400
Melting point (K)	3,000
Specific heat capacity (J/kg K)	1,100
Density (ρ) (g/cm^3)	3.1

Source: The parameters listed in this table are supplied by Goodfellow Cambridge Ltd.

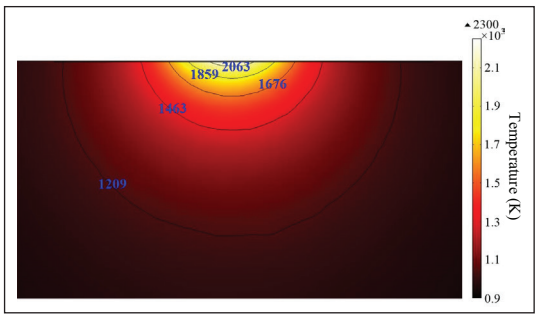

Figure 1. Thermal gradient of RB-SiC under a laser power of 80 W, wavelength of 1064 nm, and spot size of 4 mm diameter.

From Equations (10) and (13) the surface temperature can be obtained. Figure 1 shows the theoretical thermal gradient through the thickness of a workpiece 60 s after laser heating (at a laser power of 80 W). It can be seen that the maximum surface temperature of 2060 K is achieved, while the lowest temperature of 1210 K appears at a depth 10 μm below the surface, which helps to harvest the benefit of the high surface temperature without changing the integrity of the workpiece.

Experimental setup and machining conditions

To evaluate the effectiveness of LAG surface grinding, trials were carried out on a six-axis ultra-precision hybrid machine developed at the University of Strathclyde. The machine was equipped with four high-precision linear air bearing slides (full-stroke motion accuracy was better than 0.1 μm) and two rotational axes (motion accuracy better than 20 arcsec and 10 arcsec, respectively). The experimental setup on this machine is shown in Figure 2. The left vertical Z-axis carried a high-speed spindle (max spindle speed 60,000 rpm, with run-out less than 1 μm) for grinding, while the other vertical W-axis carried a fiber laser head for preheating. The laser (IPG, YLR-200-MM-AC-11) had a wavelength of 1064 nm. A focusing lens was mounted on the W-axis and connected to the laser via an optical fiber, allowing arbitrary motion between the laser spot and the workpiece. The intense laser radiation was projected peripheral to the grinding area on the RB-SiC surface in front of the engaging grinding wheel by a reflection mirror. The projected laser spot had a diameter of 4 mm.

The RB-SiC specimen, with dimensions of 12.5 mm × 12.5 mm × 5 mm (length, width, and height, respectively), was fixed on a three-component dynamometer (Kistler 9129) through a vice. A heat shield was used to insulate the heat to protect the vice and dynamometer. Resin-bonded diamond grinding wheels with a wheel diameter of 6 mm, grit size of 15 μm and 100% concentration were trued and dressed to a run-out less than 1 μm for use in the surface grinding trials.

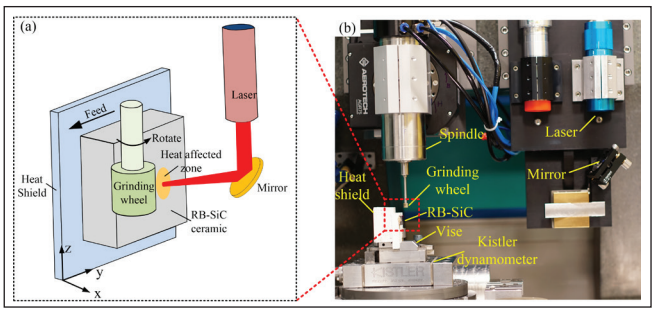

Figure 2. Laser-assisted grinding experimental setup: (a) schematic diagram of the setup and (b) hardware setup.

In the LAM trial, laser powers of 20 W, 40 W, 80 W, and 100 W were used to preheat the RB-SiC specimen for 60 s with a scanning speed of 12.5 mm/min. To fully assess the capability of the LAG process, conventional grinding trials were been performed under the same machining conditions, i.e., with a spindle speed of 8000 rpm, a feed rate of 2 mm/min at depths of cut of 5 µm, 10 µm, 15 µm, and 20 µm, respectively.

The grinding forces were measured by the dynamometer during the grinding trials. An infrared thermometer (IR-750-EUR BEHA-AMPROBE, working range of 50–1550 °C, accuracy of ±1.8%, and response time of 0.25s) was used to measure the in-line temperature of the RB-SiC surface.

The machined surface topography was inspected by a scanning electron microscope (SEM) (FEI Helios Nanolab 600i). The machined surface roughness, Ra, was measured by a white-light interferometer (Zygo CMP-200) at five different locations, with an average value as the final result. To measure the depth of subsurface damage, ion cross-section polishing was used (IB-09020CP ion polisher). To reduce random errors, four different positions were measured for each RB-SiC specimen.

Results and discussions

Surface topography

Figure 3 shows the surface topography of the ground surface in both conventional grinding and LAG. Brittle fractures were very evident on the surfaces ground by conventional grinding, but their density was reduced with a decrease in the depth of cut. The density of brittle fractures was dramatically reduced on the ground surfaces obtained by LAG. As calculated in Section 2, 80 W is very close to the required laser power. The measured surface temperature near the grinding spot was 1980K, which is very close to the calculated value shown in Figure 1. At a high temperature, material removal was predominantly in the ductile regime, while at the laser power of 100 W, the density of brittle fractures on the ground surface increased, although it was still less than 5%.

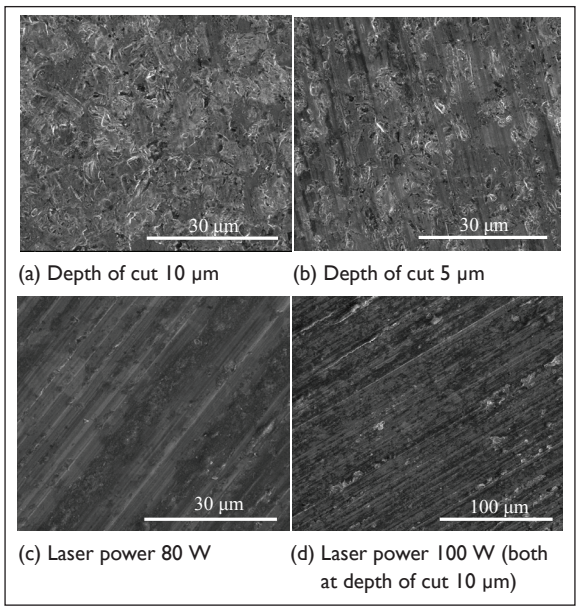

Figure 3. Surface topography of ground surfaces in both conventional grinding and laser-assisted grinding (spindle speed 8000 rpm, feed rate 2 mm/min).

The reduction of the machined surface roughness, Ra, by LAG is further confirmed by Figure 4, in which an improvement of 37%–40% is observed under the laser power of 80 W when the depth of cut varied from 5 µm to 20 µm. However, at the laser power of 20 W, there was almost no change in Ra, which indicates that the greater laser preheating was now powerful enough to soften the material. A slight reduction of surface roughness was seen at the laser power of 40 W, as laser heat started to soften the material. Figure 4 also shows that although 22%–30% improvement was achieved at the laser power of 100 W, the machined surface roughness was worse than at 80 W due to overheating. This observation was demonstrated by Vickers hardness tests. The tests showed that hardness started to drop only when the laser power was larger than 30 W. When the laser power reached 70 W, the hardness of the RB-SiC was dramatically decreased to 2480 HV from the original 2920 HV at the laser power of 20 W.[10]

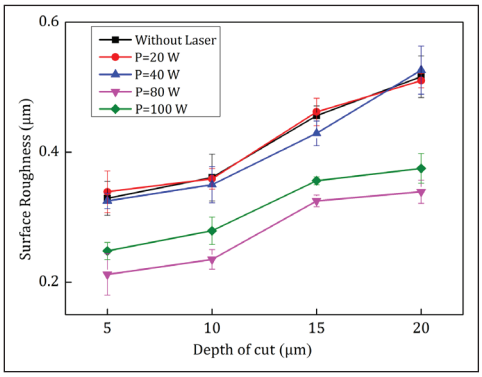

Figure 4. Comparison of attainable surface roughness Ra of the ground RB-SiC by conventional grinding and laser-assisted grinding.

Subsurface damage

Grinding-induced subsurface damage of brittle materials has been extensively studied in the past.[11,12] Material properties of fracture toughness and hardness, wheel geometry and type (grit size, geometry, bond materials, etc.), dynamic stiffness of the grinding machine, and grinding parameters can all influence the level of subsurface damage.[13,14] Figure 5 shows the comparison of subsurface damage of ground RB-SiC by conventional grinding and that by LAG at the laser power of 80 W. Very small micro-cracks were observed underneath the ground surface in a layer with depth 1.84 µm in conventional grinding with a depth of cut of 5 µm. The depth of damage was limited by the compliance provided by the resin-bonded grinding wheel. However, as the depth of cut increased, a big lateral crack appeared at 8.6 µm underneath the ground surface. When using LAG, only small micro-cracks were observed and a significant reduction of depth of subsurface damage (22%–50.6%) was achieved.

Specific energy

To further explain the effect of laser heating on subsurface damage on the ground RB-SiC, specific grinding energy, E, in the machining trial was calculated. The specific grinding energy can be described as:

$$E = \frac{F_t V_s}{a V_w b} \tag{14}$$

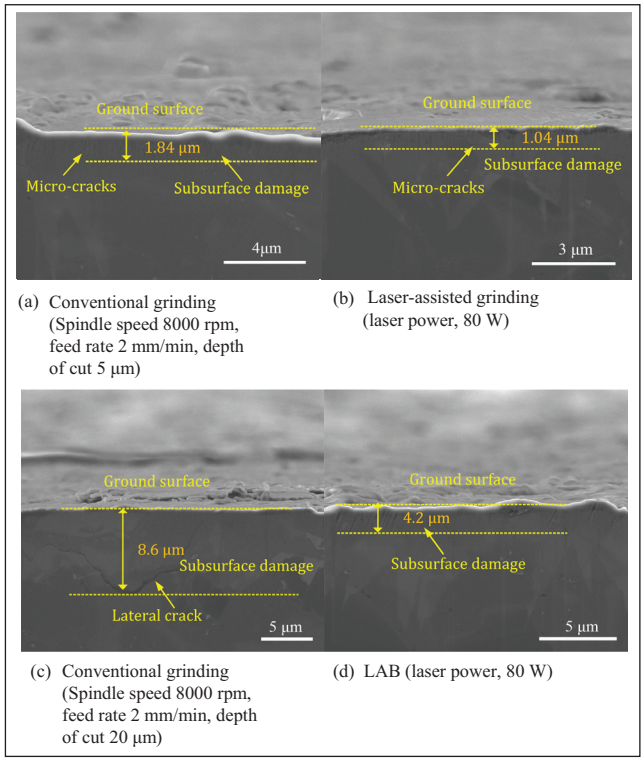

(a) Conventional grinding (Spindle speed 8000 rpm, feed rate 2 mm/min, depth of cut 5 µm)

(b) Laser-assisted grinding (laser power, 80 W)

(c) Conventional grinding (Spindle speed 8000 rpm, feed rate 2 mm/min, depth of cut 20 µm)

(d) LAB (laser power, 80 W)

Figure 5. Comparison of subsurface damage in conventional grinding and laser-assisted grinding.

where F_t, v_s, a_p, v_w, and b are the tangential grinding force, wheel speed, depth of cut, work speed, and cutting width, respectively. The material removal mechanism in grinding RB-SiC is complex. It involves both brittle fracture and plastic deformation. However, ductile-regime material removal requires higher specific energy than brittle fracture[15] as it requires more energy to initiate dislocations. Figure 6(a) illustrates the variation of specific grinding energy in the machining trials. In conventional grinding, when the depth of cut increased from 5 µm to 20 µm, the specific energy decreased from 465 J/mm^3 to 318 J/mm^3. It indicates that the material removal regime changed from predominantly ductile to predominantly brittle, as reflected in the ground surface topography shown in Figure 3. At 5 µm depth of cut, the specific grinding energy in the LAG process was increased to 712 J/mm^3 at a laser power of 80 W. The measured tangential grinding force and normal grinding force, in comparison with those in conventional grinding, are shown in Figure 6(b). It can be seen that the tangential force in the LAG process becomes profound (53% of the overall grinding force) and it is larger than that in conventional grinding (20% of the overall grinding force). It explains why specific grinding energy in the LAG process is larger than that in conventional grinding. The results show that laser preheating increases specific grinding energy. This is consistent with increasing the proportion of ductile removal. As a result, subsurface damage can be reduced.

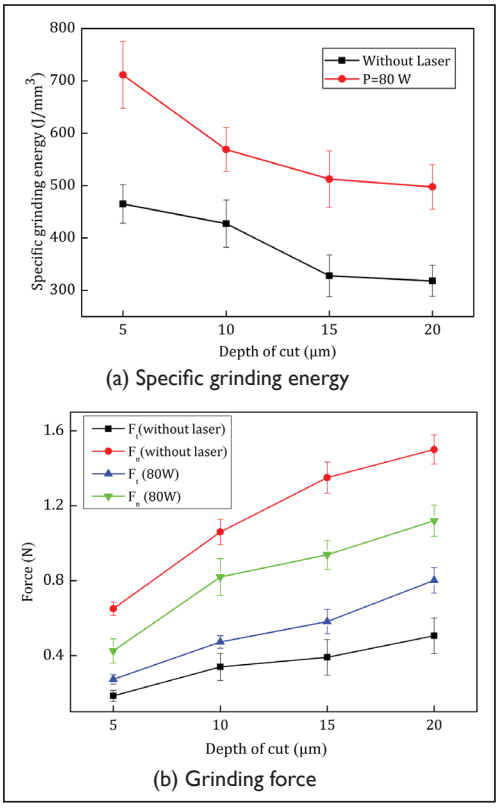

Figure 6. Specific energy and grinding force in conventional grinding and laser-assisted grinding of different laser powers at different depths of cut.

Conclusion

The article presents results for the development of LAG for RB-SiC. The following conclusions can be drawn:

- Combining the TTM and Fourier's law, the laser power for laser heating can be calculated and used to control the surface temperature and thermal gradient in order to benefit from high surface temperature in terms of reduction of hardness in a thin layer of work material without changing the integrity of the workpiece after grinding.
- LAG can significantly reduce the surface roughness and subsurface damage.
- Increase of specific energy in the LAG process can enhance the ductile-regime condition and result in low subsurface damage in ground RB-SiC.

Acknowledgements

The authors would like to thank the UK EPSRC (EP/K018345/1) and China's NKR&D programs (2016YFB1102204) and 973 (2011CB013202), and the International Cooperation Program of China (No. 2015DFA70630) for the financial support for this article.

Data statement

All data underpinning this publication are available from the University of Strathclyde Knowledge Base at https://doi.org/10.15129/d80d1509-25d0-459d-813d-c60771fe6cc2

Declaration of conflicting interests

The authors declared no potential conflicts of interest with respect to the research, authorship, and/or publication of this article.

Funding

The authors received no financial support for the research, authorship, and/or publication of this article.

ORCID iD

Xichun Luo https://orcid.org/0000-0002-5024-7058

References

1. Liang Z, Wang X, Wu Y, et al. Experimental study on brittle-ductile transition in elliptical ultrasonic assisted grinding (EUAG) of monocrystal sapphire using single diamond abrasive gran. *Int J Mach Tools Manuf* 2013; 71: 41–51.
2. Melkote S, Kumar M, Hashimoto F, et al. Laser-assisted micro milling of hard-to-machine materials. *CIRP Annals* 2009; 41/1: 45–48.
3. Chang W, Luo X, Zhao Q, et al. Laser assisted micro grinding of high strength materials. *Key Eng Mater* 2012; 496: 44–49.
4. Azarhoushang B, Soltani B, Daneshi A. Study of the effects of laser micro structuring on grinding of silicon nitride ceramics. *CIRP Annals* 2018; 67/1: 329–332.
5. Wang Y, Yang LJ, Wang NJ. An investigation of laser-assisted machining of Al_2O_3 particle reinforced aluminum matrix composite. *J Mater Process Technol* 2002; 129: 268–272.
6. Chang C, Kuo C. An investigation of laser-assisted machining of Al_2O_3 ceramics planning. *Int J Mach Tools Manuf* 2007; 47: 452–461.
7. Guerrini G, Lutey AHA, Melkote SN, et al. High throughput hybrid laser assisted machining of sintered reaction bonded silicon nitride. *J Mater Process Tech* 2018; 252: 628–635.
8. Lee S, Kim J, Suh J. Microstructural variations and machining characteristics of silicon nitride ceramics from increasing the temperature in laser assisted machining. *Int J Precis Eng Manuf* 2014; 15: 1269–1274.
9. Wellershoff S-S, Hohlfeld J, Gudde J, et al. The role of electron-phonon coupling in femtosecond laser damage of metals. *Appl Phys A Mater Sci Process* 1999; 69S: 99–107.
10. Li Z, Zhang F, Luo X, et al. Material removal mechanism of laser-assisted grinding of RB-SiC ceramics and process optimization. *J Eur Ceram Soc* 2019; 39(4): 705–717.
11. Inasaki I. Grinding of hard and brittle materials. *CIRP Annals* 1987; 36/2: 463–471.
12. Brinksmeier E, Mutlugunes Y, Klocke F, et al. Ultra-precision grinding. *CIRP Annals* 2010; 59/2: 652–671.
13. Zhang B, Howes TD. Subsurface evaluation of ground ceramics. *CIRP Annals* 1995; 44/1: 263–266.
14. Schnurbusch G, Brinksmeier E, Riemer O. Influence of cutting speed on subsurface damage morphology and distribution in ground fused silica. *Inventions* 2017; 2(3): 15.
15. Bifano TG, Fawcett SC. Specific energy as an in-process control variable for ductile-regime grinding. *Precis Eng* 1991; 13(4): 256–262.